

## An upper bound on lithosphere thickness from glacio-isostatic adjustment in Fennoscandia\*

Detlef Wolf

Geophysics Division, Geological Survey of Canada, Ottawa, Ontario, Canada, K1A 0Y3

**Abstract.** The three-layer Maxwell half-space model of the earth and a disk-load approximation of the Weichselian deglaciation history of Fennoscandia are used to calculate glacio-isostatic adjustment for this region. The calculations include the effects of deglaciation-induced geoid perturbations and eustatic sea-level rise and regard (1) lithosphere thickness, (2) asthenosphere viscosity and (3) ice thickness as the free model parameters. Numerical values of parameters (1)–(3) are estimated by calculating the past land uplift and present land-uplift rate observed in central Sweden (glaciation centre) and the past land uplift and past land tilt observed in southern Finland (glaciation margin). The uniqueness of the estimates and their sensitivity to uncertainties in (4) subasthenosphere viscosity, (5) ice cross-section and (6) deglaciation time are also assessed. The principal result of the investigation is that it suggests an upper bound of 80 km on the thickness of the Fennoscandian lithosphere.

**Key words:** Asthenosphere – Fennoscandia – Glacio-isostasy – Lithosphere – Maxwell continuum – Weichselian ice-sheet

### Introduction

The idea of interpreting the isostatic adjustment caused by the ablation of the Weichselian ice-sheet in Fennoscandia in terms of the earth's internal constitution and rheology dates back to the beginning of this century. The early investigators discussed the nature of the compensation mechanism only qualitatively (e.g. Nansen, 1921; Daly, 1934). Later, van Bemmelen and Berlage (1935) and Haskell (1935) proposed quantitative interpretations, which have been extended by many others since then (cf. Cathles, 1975).

The main purpose of these interpretations was to estimate the viscosity of the earth's mantle. The effect caused by the flexural rigidity of the earth's lithosphere (elastic surface layer) was usually neglected, although Niskanen's (1943, 1949) theoretical analyses were suggestive of the potential importance of that structural feature to glacio-isostatic adjustment in Fennoscandia.

The first attempt to determine lithosphere thickness for Fennoscandia appears to be that made by McConnell (1968). Using Sauramo's (1958) shoreline diagram, he esti-

mated the relaxation-time spectrum of the Fennoscandian uplift. The short-wavelength part of the spectrum allowed him to infer the existence of a 120-km-thick lithosphere superjacent to an asthenosphere (low-viscosity layer).

Cathles (1975, pp. 180–184) extended McConnell's (1968) interpretation and showed that there exists a trade-off between lithosphere thickness and asthenosphere viscosity so that an increase in lithosphere thickness requires an increase in asthenosphere viscosity. This agrees with Parsons' (1972, pp. 172–201) analysis, which uses Backus-Gilbert inverse theory to show that an asthenosphere is only marginally resolvable from the relaxation-time spectrum.

A necessary condition for the validity of these inferences is the accuracy of McConnell's (1968) relaxation-time spectrum. Walcott (1980) discussed this in the light of inconsistencies between several shoreline diagrams proposed for Fennoscandia and noted that the short-wavelength part of McConnell's spectrum is highly uncertain.

Cathles (1975, pp. 184–191) also used a three-layer earth model and an elementary load model to calculate land uplift for the Fennoscandian glaciation centre and land-uplift rates for a radial profile from this centre. Based on a qualitative analysis of the long-wavelength gravity field in Fennoscandia, he assumed the flexural rigidity of  $5.0 \times 10^{24}$  Nm, approximately corresponding to the thickness of 70 km, for the lithosphere in his calculations. Cathles (1975, pp. 151–154) claimed that such a flexural rigidity is too small to modify the land uplift near the Fennoscandian glaciation centre significantly. Clearly, many assumptions enter into Cathles' argument and his conclusions are, therefore, not convincing.

Considering the contingencies involved in these estimates of lithosphere thickness for Fennoscandia, a more detailed investigation of the effect of a lithosphere on glacio-isostatic adjustment appears desirable. Previous calculations showed that, near the Fennoscandian glaciation centre, the land uplift is distinctly sensitive to the presence of a lithosphere (Wolf, 1984, 1985a). However, a similarly distinct sensitivity to the presence of an asthenosphere was also indicated. This suggested the possibility of an ambiguity when interpreting the land uplift observed in central Sweden reminiscent of the ambiguity noted by Cathles (1975) when interpreting McConnell's (1968) relaxation-time spectrum. Calculations of land uplift for Ångermanland (central Sweden) confirmed that suspicion. Without an asthenosphere, a lithosphere thickness of about 200 km was compatible with the observations; with an asthenosphere of ap-

\* Geological Survey of Canada Contribution No. 35,386

appropriate viscosity and the ice thickness suitably reduced, a lithosphere thickness of about 100 km was required (Wolf, 1986a). The uplift observations in Ångermanland were thus found to be insufficient for determining lithosphere thickness, asthenosphere viscosity and ice thickness uniquely.

The question of the thickness of the Fennoscandian lithosphere was, therefore, addressed in a different way, and a heuristic method of estimating that parameter was developed. It is based on a static earth model in which the lithosphere is assumed to be elastic and the sublithosphere to be inviscid. If land uplift and tilt near the load margin are known, the method allows the direct calculation of lithosphere thickness. The method was applied to observations of land uplift and land tilt in southern Finland and yielded an upper bound of  $110 \pm 30$  km on the thickness of the Fennoscandian lithosphere (Wolf, 1986b).

The present study endeavours to improve that thickness estimate by using the three-layer Maxwell half-space model of the earth and a disk-load approximation of the Fennoscandian deglaciation history, with (1) lithosphere thickness, (2) asthenosphere viscosity and (3) ice thickness being the free parameters. In contrast to Wolf (1986a), the effect of deglaciation-induced geoid perturbations has been taken into account and the load model has been improved. The latter is necessary to calculate the land adjustment both for the centre and the margin of the Fennoscandian ice-sheet. The uniqueness of the set of numerical values inferred for the parameters (1)–(3) above and their sensitivity to uncertainties in (4) subasthenosphere viscosity, (5) ice cross-section and (6) deglaciation time are also assessed. This leads to an improved upper bound on the thickness of the Fennoscandian lithosphere.

### Theoretical model

The present study uses the externally gravitating, layered, incompressible Maxwell half-space (Wolf, 1985a) as the earth model. The interpretation of glacio-isostatic uplift in terms of earth structure requires the calculation of the load-induced (downward) displacement component,  $w$ . Let  $q(r)$  denote the axisymmetric pressure at the radial distance  $r$  caused by the impulsive loading event  $\delta(t)$  at the time  $t=0$ . Then, in the wave-number domain,

$$\hat{w}(k, z_l, t) = W^{(ve)}(k, z_l, t) \hat{q}(k), \quad (1)$$

where the circumflex denotes zeroth-order Hankel transformation of the associated variable with respect to  $r$ ,  $k$  the (horizontal) wave number (Hankel-transform variable) and  $z_l$  the depth to the top of the  $l$ -th layer below the surface. The impulse transfer function for displacement,  $W^{(ve)}$ , also depends on the parameters characterizing each layer  $l$ , viz. thickness  $h_l$ , density  $\rho_l$ , rigidity  $\mu_l$  and viscosity  $\eta_l$  (cf. Wolf, 1985a).

A more accurate interpretation of uplift also requires the calculation of the deglaciation-induced geopotential perturbation,  $\delta U$ . Since the Maxwell continuum is assumed to be incompressible,  $\delta U$  satisfies Laplace's equation. In the Hankel-transform domain, therefore,

$$\delta \hat{U}''(k, z, t) - k^2 \delta \hat{U}(k, z, t) = 0 \quad (2)$$

subject to the boundary conditions

$$\delta \hat{U}(k, z_1 + 0, t) - \delta \hat{U}(k, z_1 - 0, t) = 0 \quad (3)$$

Table 1. Parameters of earth model A.1

$l$	$h_l$ (km)	$\rho_l$ (kg m <sup>-3</sup> )	$\mu_l$ (Pa)	$\eta_l$ (Pa s)
1	$h_1$	3,380	$0.67 \times 10^{11}$	$\infty$
2	100	3,380	$0.67 \times 10^{11}$	$\eta_2$
3	$\infty$	3,380	$1.45 \times 10^{11}$	$1.0 \times 10^{21}$

and

$$\delta \hat{U}'(k, z_l + 0, t) - \delta \hat{U}'(k, z_l - 0, t) = 4\pi\gamma \hat{\kappa}_l(k, t). \quad (4)$$

The prime denotes differentiation with respect to  $z$ ;  $\gamma$  is the gravitational constant. The Hankel-transformed interface-mass density,  $\hat{\kappa}_l$ , is given by

$$\hat{\kappa}_l(k, t) = -\hat{q}(k) \begin{cases} (\rho_l - \rho_{l-1}) W^{(ve)}(k, z_l, t) - \delta(t)/g, & l=1 \\ (\rho_l - \rho_{l-1}) W^{(ve)}(k, z_l, t), & l>1 \end{cases} \quad (5)$$

with  $g$  the gravitational acceleration. By Eq. (1),  $-\hat{q}(\rho_l - \rho_{l-1}) W^{(ve)}$  is the part of  $\hat{\kappa}_l$  associated with the interface deflection;  $\hat{q}\delta(t)/g$  is the part associated with the load. Assuming also  $\lim_{|z| \rightarrow \infty} \delta \hat{U} = 0$ , the solution at  $z = z_1$  is

$$\delta \hat{U}(k, z_1, t) = G^{(ve)}(k, z_1, t) \hat{q}(k), \quad (6)$$

where

$$G^{(ve)}(k, z_1, t) = \frac{2\pi\gamma}{k} \sum_{i=1}^L \{(\rho_i - \rho_{i-1}) W^{(ve)}(k, z_i, t) \times \exp[-k(z_1 - z_i)]\} - \frac{2\pi\gamma}{k} \frac{\delta(t)}{g}. \quad (7)$$

This is the impulse transfer function for potential. For the Hankel-transformed (downward) geoid perturbation,  $\hat{\varepsilon}$ , therefore,

$$\hat{\varepsilon}(k, z_1, t) = \frac{1}{g} G^{(ve)}(k, z_1, t) \hat{q}(k). \quad (8)$$

The higher-order geoid perturbations caused by the redistribution of ocean water according to Eq. (8) (e.g. Farrell and Clark, 1976) will be neglected here.

As in Wolf (1986a), the three-layer earth model A.1 (Table 1) is considered, with  $h_1$  and  $\eta_2$  as free parameters. Alternatively,  $h_2$  rather than  $\eta_2$  could have been selected as a free parameter. However, as long as  $h_2$  is small compared with the lateral dimensions of the load, the response of the asthenosphere is approximately governed by the single parameter  $D = \eta_2 h_2^2/3$  (e.g. Nadai, 1963, pp. 260–262, 285–287), i.e. the two situations are equivalent. The numerical values of  $\rho_l$  and  $\mu_l$  are taken from a simple elastic earth model (Bullen, 1963, pp. 232–235); the value of  $1.0 \times 10^{21}$  Pa s for  $\eta_3$  is the upper-mantle value of several viscous earth models (e.g. Cathles, 1975; Peltier and Andrews, 1976; Wu and Peltier, 1983). The effect of increasing  $\eta_3$  to  $2.0 \times 10^{21}$  Pa s (earth model A.1a) is also investigated. Such a viscosity value may be required for the lower mantle to explain the deglaciation-induced part of the free-air gravity anomalies observed in Fennoscandia and Laurentia (Wu and Peltier, 1983; Wolf, 1986a).

**Table 2.** Parameters of load model WEICHSEL-1 ( $h_{0,n}^2/R_n = \text{const.}$ ,  $\rho = 910 \text{ kg m}^{-3}$ ; 0 B.P. = A.D. 1950)

$n$	$t_{1,n}$ (ka B.P.)	$t_{2,n}$ (ka B.P.)	$x_n$ (km)	$y_n$ (km)	$R_n$ (km)
1	100.0	18.0	-325	0	900
2	18.0	17.0	-375	0	850
3	17.0	16.0	-425	0	800
4	16.0	15.0	-475	0	750
5	15.0	14.0	-525	0	700
6	14.0	13.0	-575	0	650
7	13.0	11.0	-625	0	600
8	11.0	9.8	-625	0	500
9	9.8	9.6	-625	0	400
10	9.6	9.4	-625	0	300
11	9.4	9.2	-625	0	200
12	9.2	9.0	-625	0	100

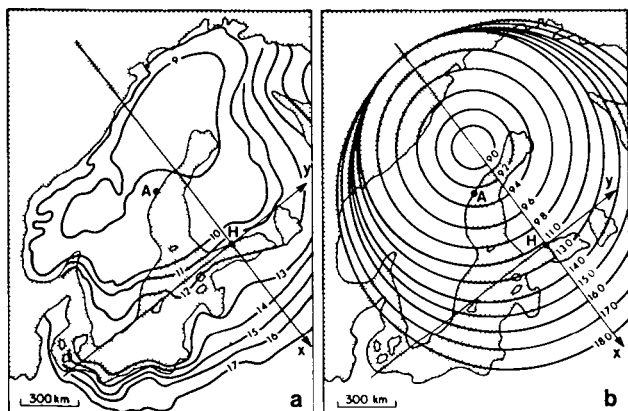


**Fig. 1a, b.** a Observed (after de Geer, 1954; cf. also Andersen, 1981) and b schematic (load model WEICHSEL-1) deglaciation isochrons (in units of ka B.P.); the symbols *A* and *H* denote Ångermanland and Helsinki, respectively

The present study uses load model WEICHSEL-1 (Fig. 1 b, Table 2). It is characterized by a sequence of box-car loading functions,  $H(t-t_{1,n})-H(t-t_{2,n})$ , where  $H$  denotes the Heaviside function. In addition, load model WEICHSEL-1a, for which the sequence of loading functions is shifted in time by  $-1$  ka, is considered. (A positive shift would entail a conflict between deglaciation and emergence chronologies). With  $\hat{q}_n$  the Hankel-transformed load pressure associated with the  $n$ -th box-car loading function, therefore, instead of Eqs. (1) and (8),

$$\hat{w}(k, z_1, t) = W_n^{(ve)}(k, z_1, t) \hat{q}_n(k), \quad (9)$$

and

$$\hat{\varepsilon}(k, z_1, t) = \frac{1}{g} G_n^{(ve)}(k, z_1, t) \hat{q}_n(k). \quad (10)$$

The  $n$ -th box-car transfer functions for displacement and potential,  $W_n^{(ve)}$  and  $G_n^{(ve)}$ , respectively, are obtained by convolution (Appendix A).

Since  $q_n$  is assumed to be axisymmetric and the load density  $\rho$  to be constant, the load cross-section is also axisymmetric. Here, disk loads of radius  $R_n$  and centered at the source point  $(x_n, y_n)$  (Fig. 1 b, Table 2) are considered.

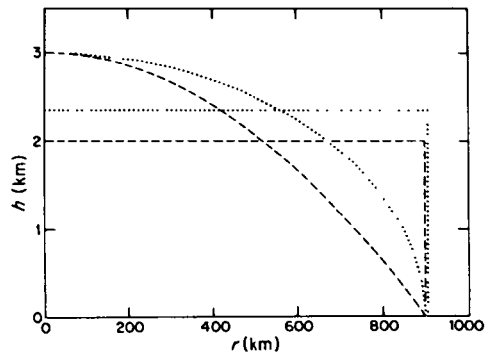


**Fig. 2.** Load thickness  $h$  as a function of radial distance  $r$  for an axisymmetric load of parabolic (dashed) or elliptic (dotted) cross-section; the straight lines represent equal-area rectangular cross-sections

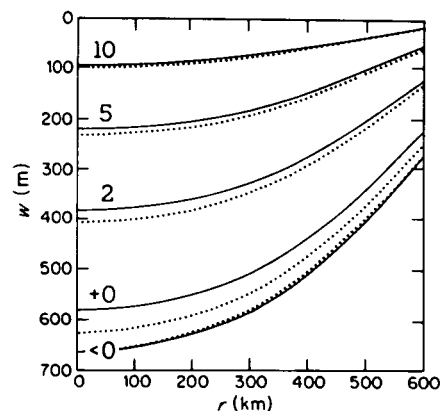


**Fig. 3.** Vertical surface displacement  $w$  with respect to the geoid (solid) or with respect to the horizontal plane (dotted) as a function of radial distance  $r$  from the load axis for several times (in units of ka) after a Heaviside unloading event; the calculations apply to earth model A.1 with  $h_1 = 100$  km and  $\eta_2 = 1.0 \times 10^{21}$  Pa s, and to an axisymmetric load of rectangular cross-section with  $h = 2$  km,  $R = 600$  km and  $\rho = 1,000 \text{ kg m}^{-3}$

The whole sequence is intended to approximate the Fennoscandian deglaciation history (Fig. 1 a). The axial load thickness for the first loading function,  $h_{0,1}$ , is taken as a free parameter; however, the ratio  $h_{0,n}^2/R_n$  is assumed to be independent of  $n$ . This partial restriction is in accordance with the theory of perfectly plastic ice-sheets at equilibrium (Orowan, 1949; cf. also Paterson, 1981, p. 154). In the present study, *parabolic* and, in addition, *elliptic* load cross-sections are considered. Compared with the parabolic cross-section, the elliptic cross-section is characterized by steeper slopes near the load margin (Fig. 2). Not considered is the *theoretical* profile of a perfectly plastic ice-sheet at equilibrium (Nye, 1952; cf. also Paterson, 1981, pp. 153–164), which is somewhat intermediate between the parabolic and elliptic profiles. Substitution of the appropriate Hankel transforms for  $\hat{q}_n$  in Eqs. (9) and (10), inverse Hankel transformation and superposition of the solutions for the individual box-car loading functions yields the final solutions  $w(x, y, z_1, t)$  and  $\varepsilon(x, y, z_1, t)$  for the observation point  $(x, y)$  (Appendix B).

To study the importance of geoid perturbations to the interpretation of the glacio-isostatic adjustment of Fennoscandia, it is sufficient to consider a simpler load model, viz. the Heaviside unloading event  $1-H(t)$  produced by an axisymmetric load of *rectangular* cross-section, and to

compare  $w$  with  $w - \varepsilon$  on a radial profile from the load axis for different times after unloading. Figure 3 shows that, before unloading, the geoid is almost unperturbed, i.e. the mass excess associated with  $q$  is largely compensated by the mass deficit associated with  $w$ . The small degree of upwarping of the geoid is caused by the flexural rigidity of the lithosphere, which prevents perfect local compensation. After unloading, the surface depression entails a geoid depression which decays with the surface depression. Although  $\varepsilon$  is always less than 10% of  $w$ , its magnitude may be significant at times shortly after unloading. Wu and Pelletier (1983) and Wolf (1986c) discussed other numerical examples of the effect of deglaciation-induced geoid perturbations.

The interpretation of glacio-isostatic adjustment requires the calculation of the land uplift with respect to the geoid for the time interval  $[t, 0]$ , viz.

$$H(x, y, t) = H_w(x, y, t) - H_e(x, y, t), \quad (11)$$

where the land uplift with respect to the horizontal surface,  $H_w$ , and the geoid uplift,  $H_e$ , are defined by

$$H_w(x, y, t) = w(x, y, z_1, t) - w(x, y, z_1, 0) \quad (12)$$

and

$$H_e(x, y, t) = \varepsilon(x, y, z_1, t) - \varepsilon(x, y, z_1, 0). \quad (13)$$

Let  $H_s$  denote the land emergence (land uplift with respect to the sea level) and  $H_e$  the eustatic sea-level rise (e.g. Walcott, 1972) during  $[t, 0]$ . Then the *observed* land uplift with respect to the geoid is given by

$$H(x, y, t) = H_s(x, y, t) - H_e(x, y, t), \quad (14)$$

which may be compared with the *calculated* land uplift with respect to the geoid, Eq. (11).

### Interpretation

The interpretation uses the past land emergence,  $H_s(t)$ , observed in Ångermanland and near Helsinki (Table 3). The Ångermanland observations apply to  $x = -425$  km,  $y = -150$  km (Fig. 1) and are taken from Niskanen (1939), but are originally due to Lidén (1938). The Helsinki observations apply to  $x = 0$  km,  $y = 0$  km (Fig. 1) and are estimated from emergence diagrams compiled by Donner (1980) and Eronen (1983). To obtain the observed value of  $H(t)$ ,  $H_e(t)$  must be known. Andrews (1970, pp. 22–24) suggested a quadratic function that closely approximates the mean of several eustatic corrections proposed. Here a simpler approximation is used, viz.

$$H_e(t) = \begin{cases} 0, & t \leq 6 \\ 10(t - 6), & t > 6 \end{cases} \quad (15)$$

where  $H_e$  and  $t$  must be in units of m and ka B.P., respectively (cf. also Table 3).

The ages of the emerged beaches in Ångermanland were inferred using wave chronology. The relative ages are, therefore, very accurate, but the absolute ages may be less so. Also, older beaches were mapped about 100 km inland of the location of the younger beaches (cf. Niskanen, 1939), which leads to uncertainties in  $H_s$ . Donner's (1980) and

**Table 3.** Observed land emergence  $H_s$  and observed land uplift  $H$  at  $x = -425$  km,  $y = -150$  km (Ångermanland) and at  $x = 0$  km,  $y = 0$  km (Helsinki); 0 B.P. = A.D. 1950

Ångermanland (Lidén, 1938)			Helsinki (Donner, 1980; Eronen, 1983)		
$t$ (ka B.P.)	$H_s$ (m)	$H$ (m)	$t$ (ka B.P.)	$H_s$ (m)	$H$ (m)
8.893	232	261	10.0	70	110
8.755	220	248	9.0	46	76
8.550	193	219	8.0	35	55
7.655	138.9	156	7.0	34	44
6.452	104.1	109	6.0	32	32
5.879	90.4	90	5.0	27	27
5.424	80.2	80	4.0	22	22
5.246	76.2	76	3.0	17	17
4.065	54.1	54	2.0	11	11
3.805	51.1	51	1.0	5	5
3.629	48.2	48	0.0	0	0
3.119	40.7	41			
2.076	26.3	26			
1.490	18.0	18			
1.028	12.2	12			
0.011	0.0	0			

Eronen's (1983) emergence diagrams for Helsinki compile observations obtained by different methods, which makes estimates of the uncertainties difficult. The present study assumes  $t$  to be accurate but assigns uncertainties of  $\pm 15$  m and  $\pm 10$  m to  $H$  for Ångermanland and Helsinki, respectively. These values also take into account the uncertainty in  $H_e$ .

The observed past land tilt,  $H' \equiv dH/dx$ , is estimated from shoreline diagrams (Donner, 1980; Eronen, 1983) and applies to  $x = -50$  km,  $y = 0$  km (Fig. 1). Since the construction of shoreline diagrams for Fennoscandia is, to some extent, interpretative (cf. Hyvärinen and Eronen, 1979), the liberal estimate of  $\pm 0.05 \times 10^{-3}$  is used for the uncertainty in  $H'$ .

The observed present land-uplift rates,  $\dot{H} \equiv dH/dt$ , apply to the profile connecting Helsinki and the glaciation centre (Fig. 1). The numerical values are interpolated from a smoothed contour map by Balling (1980). The original observations were obtained by precise re-levellings tied to mareograph recordings (Kääriäinen, 1966). The assumed uncertainty of  $\pm 1$  mm  $a^{-1}$  is sufficiently large to account for potentially continuing eustatic sea-level changes.

Figure 4 shows the observations of  $H$  in Ångermanland and near Helsinki, the observations of  $\dot{H}$  on the profile connecting Helsinki with the glaciation centre and the observations of  $H'$  near Helsinki. The calculations apply to earth model A.1 and WEICHSEL-1 with parabolic load cross-section. The curve-fitting process has been facilitated by the following: (1) The parameter  $h_1$  mainly determines the ratio between the calculated values of  $H(t = 8.893$  ka B.P.) for Ångermanland and of  $H(t = 10$  ka B.P.) for Helsinki, whereas  $h_{0,1}$  determines the magnitude of these values. (2) The parameter  $\eta_2$  controls the calculated value of  $\dot{H}(x = -600$  km). (3) The observations of  $H'$  near Helsinki provide little additional information, although the fact that the observed values of both  $H$  and  $H'$  can be closely fitted at the glaciation margin indicates that the parabolic cross-

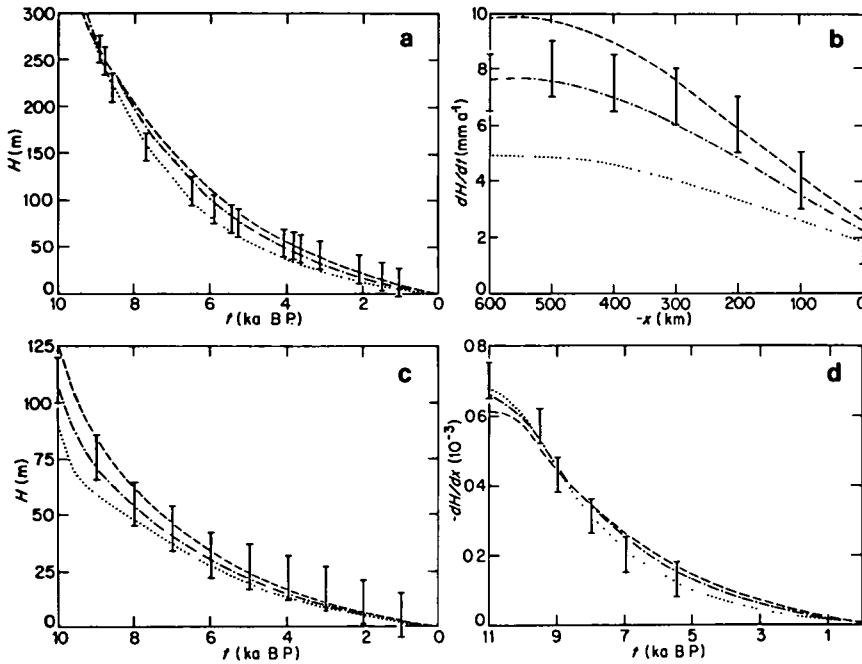


**Fig. 4a–d.** a Observed (Lidén, 1938) and calculated land uplift  $H$  for Ångermanland since time  $t$ . b Observed (Balling, 1980) and calculated land-uplift rate  $dH/dt$  as a function of distance  $x$ . c Observed (Donner, 1980; Eronen, 1983) and calculated land uplift  $H$  for Helsinki since time  $t$ . d Observed (Donner, 1980; Eronen, 1983) and calculated land tilt  $dH/dx$  for Helsinki since time  $t$ . The observations are represented by vertical bars; the calculations are represented by curves and apply to earth model A.1 with  $h_1 = 50$  km and  $\eta_2 = 7.0 \times 10^{18}$  Pa s (dotted),  $\eta_2 = 1.2 \times 10^{19}$  Pa s (dot-dashed) or  $\eta_2 = 2.0 \times 10^{19}$  Pa s (dashed), and to WEICHSEL-1 with parabolic load cross-section and  $h_{0,1} = 2.1$  km

section used cannot be grossly wrong (Wolf, 1986b). The numerical values of the free model parameters inferred in this manner are  $h_1 \cong 50$  km,  $\eta_2 \cong 1.2 \times 10^{19}$  Pa s (dot-dashed line) and  $h_{0,1} \cong 2.1$  km.

The discussion of Fig. 4 suggests that the observations used are sufficiently independent to regard the numerical values inferred for  $h_1$ ,  $\eta_2$  and  $h_{0,1}$  as being mainly imposed by the observations rather than merely reflecting certain characteristics of the theoretical model. To confirm this expectation and, in particular, to answer the related question of the uniqueness of the numerical value inferred for  $h_1$ , a more careful analysis is warranted.

To identify potential trade-offs with ease, the full set of observations shown in Fig. 4 must be reduced. Some consideration suggests that  $H(t = 8.893 \text{ ka B.P.}) = 261 \pm 15$  m (Ångermanland),  $H(t = 10 \text{ ka B.P.}) = 110 \pm 10$  m (Helsinki),  $\dot{H}(x = -600 \text{ km}) = 7.5 \pm 1.0 \text{ mm a}^{-1}$  and  $\dot{H}(t = 11 \text{ ka B.P.}) = 0.70 \pm 0.05 \times 10^{-3}$  constitute a representative subset. Figures 5–7 use this subset to study the possibility of trade-offs between  $h_1$ ,  $\eta_2$  and  $h_{0,1}$  and to investigate the sensitivity of the numerical values inferred for these parameters to uncertainties in several of the fixed model parameters.

The dashed lines of Fig. 5 apply to earth model A.1 and WEICHSEL-1 with parabolic load cross-section. For each numerical value of  $h_1$  distinguished by a solid square,  $h_{0,1}$  and  $\eta_2$  have been adjusted to achieve a perfect fit to the observed values of  $H$  in Ångermanland (Fig. 5c) and of  $\dot{H}$  (Fig. 5d). Figure 5a and b shows that this requires  $h_{0,1}$  and  $\eta_2$  to increase with increasing  $h_1$ . The increase in  $h_{0,1}$  balances most of the effect of increasing  $h_1$ ; the adjustment of  $\eta_2$  is required to fit the calculated to the observed values of  $\dot{H}$ . Figure 5a–d confirms the previous conclusion that  $h_1$  is not uniquely determined by observations of  $H$  and  $\dot{H}$  near the Fennoscandian glaciation centre alone (Wolf, 1986a). Figure 5e shows that resolution increases sharply if the observation of  $H$  near Helsinki is included as an additional constraint. Clearly, earth models with  $h_1 \geq 70$  km are now rejected. Figure 5f suggests that

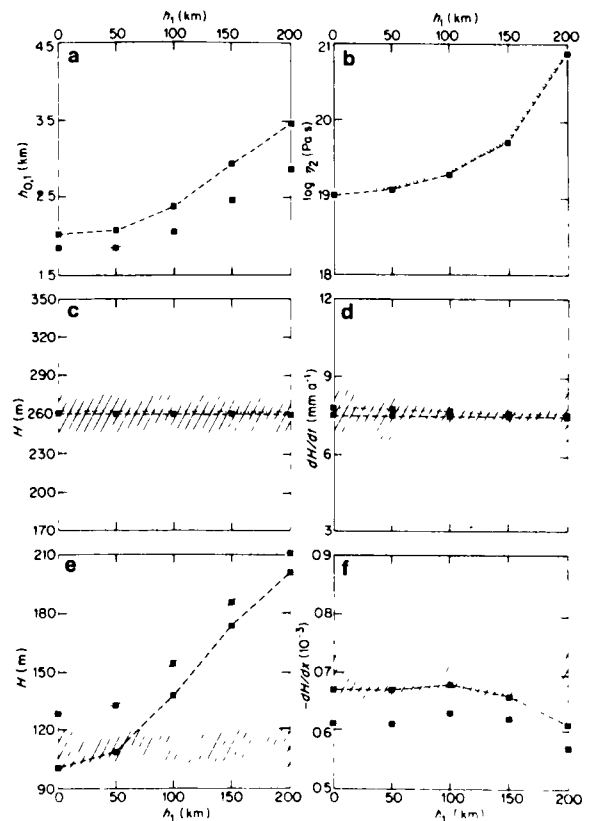


**Fig. 5a–f.** a Axial load thickness  $h_{0,1}$  and b asthenosphere viscosity  $\eta_2$  as functions of lithosphere thickness  $h_1$ ; the parameters  $h_{0,1}$  and  $\eta_2$  have been adjusted in order that the calculated values (solid squares connected by straight lines) of c land uplift  $H$  and d land-uplift rate  $dH/dt$  for central Sweden fit the observed values (hatched bands). The calculated and observed values of land uplift  $H$  and land tilt  $dH/dx$  for southern Finland are shown in e and f. The calculations apply to earth model A.1 and to WEICHSEL-1 with parabolic (dashed) or elliptical (dotted) load cross-section

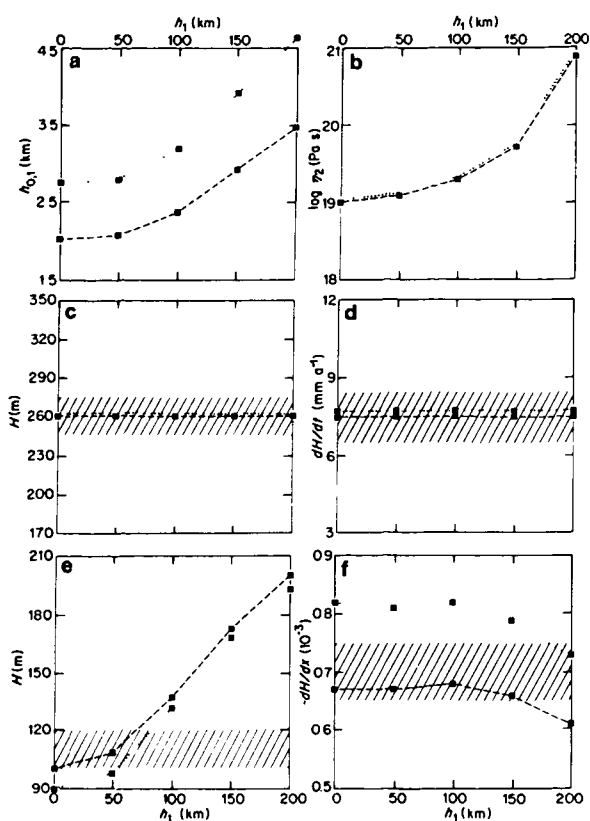


Fig. 6a-f. As for Fig. 5 except that dotted lines apply to earth model A.1 and to WEICHSEL-1a with parabolic load cross-section

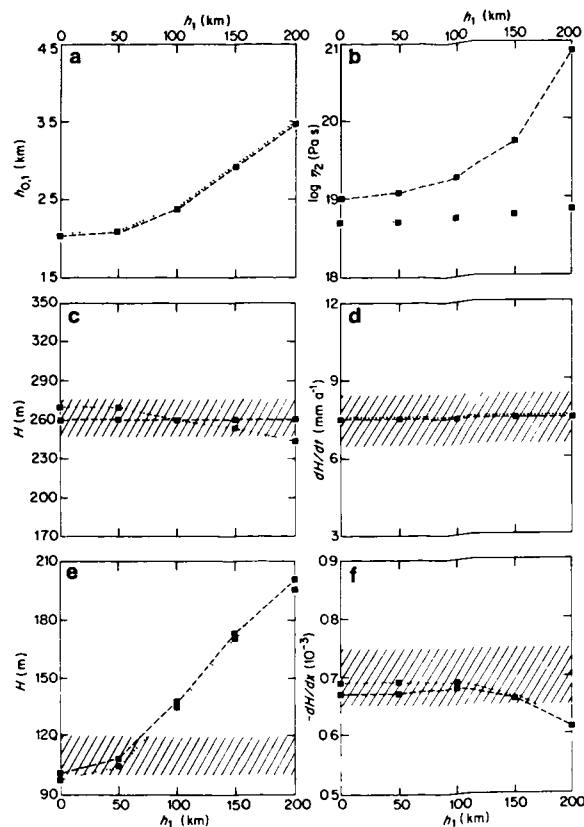


Fig. 7a-f. As for Fig. 5 except that dotted lines apply to earth model A.1a and to WEICHSEL-1 with parabolic load cross-section

the parabolic cross-section used is compatible with the observations; apart from that,  $H'$  is not very diagnostic.

The dotted lines in Fig. 5 apply to earth model A.1 and WEICHSEL-1 with elliptic load cross-section. The average thickness of this cross-section is larger than that of the parabolic cross-section by about 18% (Fig. 3). Figure 5a-d shows that a reduction in  $h_{0,1}$  for the elliptic cross-section by a comparable amount permits a perfect fit of the calculated to the observed values of  $H$  for Ångermanland. The remaining misfit between the calculated and observed values of  $\dot{H}$  is insignificant. The land adjustment near the Fennoscandian glaciation centre is, therefore, sensitive mainly to mean load thickness, i.e. it does not permit the resolution of the load profile. Figure 5e shows that the calculated values of  $H$  for Helsinki are larger for the elliptic than for the parabolic cross-section. Since the marginal load thicknesses are also larger for the elliptic than for the parabolic cross-section, it follows that, near the Fennoscandian glaciation margin,  $H$  is sensitive mainly to local rather than mean load thickness. The reduction in the calculated value of  $H'$  for the elliptic cross-section (Fig. 5f) is similarly related to the more uniform distribution of load thickness for this cross-section. The failure of WEICHSEL-1 with elliptic load cross-section to fit the calculated to the observed values of  $H$  and  $H'$  near the glaciation margin even for small values of  $h_1$  indicates that this cross-section is not completely adequate. For small values of  $h_1$ , the discrepancy is, however, not severe and the point should not be over-emphasized.

The dashed lines of Fig. 6 again apply to earth model A.1 and WEICHSEL-1 with parabolic load cross-section.

The dotted lines, however, are for WEICHSEL-1a. The comparison of the two sets of calculations, therefore, shows the sensitivity of the numerical values inferred for  $h_1$ ,  $\eta_2$  and  $h_{0,1}$  to a shift of the sequence of loading functions by  $-1$  ka. This extends the time elapsed since unloading by 1 ka. Near the glaciation centre, the resulting reduction in the calculated values of  $H$  and  $\dot{H}$  can be simply balanced by an increase in  $h_{0,1}$  (Fig. 6a-d). As before, a perfect fit of the calculated to the observed values of  $H$  has been forced for Ångermanland. The remaining misfit between the calculated and observed values of  $\dot{H}$  is small compared with the uncertainty assumed for the observation. Figure 6e shows that WEICHSEL-1a slightly reduces the calculated values of  $H$  for Helsinki. This entails that the maximum value of  $h_1$  compatible with the observation increases to about 80 km. The discrepancies between the calculated and observed values of  $H'$  for such values of  $h_1$  are, however, larger by a factor of about 2 than the uncertainty assumed for the observation (Fig. 6f).

Figure 7 investigates the modifications of the results for earth model A.1 and WEICHSEL-1 with parabolic load cross-section (dashed lines) introduced by using earth model A.1a (dotted lines) instead. Thus, the sensitivity of the numerical values inferred for  $h_1$ ,  $\eta_2$  and  $h_{0,1}$  to an increase in  $\eta_3$  to  $2.0 \times 10^{21}$  Pa s is studied. Figure 7a-d shows that, for the glaciation centre, there exists a trade-off between  $\eta_2$  and  $\eta_3$  so that the increase in  $\eta_3$  can be largely compensated by a suitable decrease in  $\eta_2$ . Since  $\dot{H}$  was found to be highly diagnostic of the viscosity structure (Fig. 4b), a perfect fit has been forced for  $\dot{H}$ . The remaining misfit be-

tween the calculated and observed values of  $H$  for Ångermanland is tolerable considering the uncertainty of the observation. Figure 7e and f shows that this trade-off between  $\eta_2$  and  $\eta_3$  also leaves the calculated values for the glaciation margin essentially unchanged. The maximum value of  $h_1$  compatible with the observed value of  $H$  near Helsinki is about 75 km.

## Discussion and conclusion

The interpretation of the glacio-isostatic adjustment of Fennoscandia and the analysis of the uniqueness of the set of numerical values inferred for the free model parameters can be summarized as follows:

(1) The observations of  $H$  and  $\dot{H}$  in central Sweden and of  $H$  and  $H'$  in southern Finland can be explained by the basic model, i.e. earth model A.1 and WEICHSEL-1 with parabolic load cross-section, if  $h_1 \cong 50$  km,  $\eta_2 \cong 1.2 \times 10^{19}$  Pa s and  $h_{0,1} \cong 2.1$  km.

(2) The simultaneous calculation of  $H(t=8.893$  ka B.P.) for Ångermanland and of  $H(t=10$  ka B.P.) for Helsinki for different values of  $h_1$  shows that  $h_1 \geq 70$  km is rejected by the observations. For  $h_1 \leq 70$  km, the sensitivity to  $h_1$  is weak. Therefore, only an upper bound can be inferred from the observations.

(3) The modification of the basic model by an elliptic load cross-section leads to values of  $H$  and  $H'$  for southern Finland outside the uncertainties of the observations for any numerical value of  $h_1$ .

(4) The modification of the basic model by a shift of the sequence of loading functions by  $-1$  ka (WEICHSEL-1a) increases the maximum value of  $h_1$  compatible with the observations to about 80 km. Also, an increase in  $h_{0,1}$  to about 2.8 km is required whereas  $\eta_2$  remains unchanged. However, the values of  $H'$  tend to be too large.

(5) The modification of the basic model by a two-fold increase in  $\eta_3$  (earth model A.1a) entails a decrease in  $\eta_2$  to about  $5.3 \times 10^{18}$  Pa s but only insignificant changes in  $h_1$  and  $h_{0,1}$ .

The upper bound of about 80 km found for  $h_1$  is very similar to Cathles' (1975) estimate of this parameter. However, as discussed previously (Wolf, 1986a) and also shown here, the limited set of observations used by Cathles did not allow him to resolve the numerical value of  $h_1$ . The coincidence is, therefore, largely fortuitous.

The estimate of  $h_1$  for the Fennoscandian lithosphere may be contrasted with estimates of this parameter for the Laurentian lithosphere from observations of land adjustment after the ablation of the Wisconsin Laurentide ice-sheet. Walcott (1970) and Wolf (1985b) used observations of land tilt near the Laurentide glaciation margin and inferred numerical values of  $h_1$  which are very similar to the upper bound of 80 km obtained for Fennoscandia. Peltier (1984) used observations of land emergence along the North American east coast and estimated  $h_1 \cong 200$  km for the Laurentian lithosphere.

Recently, Sabadini et al. (1986) studied the effects of upper-mantle lateral heterogeneities likely to be associated with a passive continental margin on the land uplift following the disappearance of a Laurentide-sized load. They showed that interpretations of the observed land uplift for points close to both the continental margin and the glaciation margin results in underestimates of  $h_1$  for the continen-

tal lithosphere if the lateral heterogeneity is neglected. Discussing Peltier's (1984) study in this context, Sabadini et al. concluded that  $h_1 \geq 250$  km would be required for the Laurentian lithosphere if the Atlantic continental margin were accounted for. This is much higher than any other estimate of  $h_1$  inferred for Laurentia or Fennoscandia, and ways of reconciling the divergent estimates are needed.

For Fennoscandia, the problem of lateral upper-mantle heterogeneity is less severe. The observation points in central Sweden and, in particular, southern Finland are well removed from the continental margin, and a laterally homogeneous model appears to be an adequate approximation.

Finally, the question as to what extent the upper bound on  $h_1$  reflects the approximations of the load model used must be briefly addressed. Clearly, WEICHSEL-1 does not accurately model the Fennoscandian deglaciation history (Fig. 1), nor does it allow for the necessarily gradual ice accumulation before deglaciation. However, since the accuracy of WEICHSEL-1 is highest at locations and times close to those of the observations, and since the calculated response at a particular location and time is predominantly caused by the spatially and temporally adjacent parts of the load, WEICHSEL-1 is not expected to result in significant bias.

Quinlan and Beaumont (1982) have recently proposed a method of improving the model of the Laurentide ice-sheet. Using ICE-1 (Peltier and Andrews, 1976) as the starting model in a detailed interpretation of the post-glacial emergence of the Canadian east coast, they determined to which features of the load the calculated response at the locations and times of the observations is most sensitive. This led to the construction of a modified version of ICE-1, which has enhanced accuracy in these crucial features and gives a better fit to the emergence observations.

In future interpretations of the Fennoscandian uplift, more observations should be considered. Then, however, WEICHSEL-1 may become inadequate and require modification. Clearly, the method of Quinlan and Beaumont (1982) offers itself for refining WEICHSEL-1. The so improved load model may later be used to arrive also at improved estimates of the parameters of the earth model.

## Appendix A

### Convolution of impulse transfer function

For the layered Maxwell half-space and an arbitrary field quantity, the impulse transfer function,  $T^{(v,e)}$ , is given by (Wolf, 1985a)

$$T^{(v,e)}(k, z_l, t) = T^{(e)}(k, z_l) \delta(t) + \sum_{m=1}^M T_m^{(v)}(k, z_l) s_m(k) \exp[-s_m(k)t], \quad (16)$$

where  $T^{(e)}$  is the elastic transfer function and  $T_m^{(v)}$  is the  $m$ -th viscous transfer function (eigenfunction) belonging to the  $m$ -th inverse relaxation time (eigenvalue)  $s_m$ . The functional forms of  $T^{(e)}$ ,  $T_m^{(v)}$  and  $s_m$ , and the number of modes,  $M$ , depend on the type of layering considered. Since the Maxwell rheology is linear, the response to the box-car loading function  $H(t-t_{1,n}) - H(t-t_{2,n})$  is obtained by convolution, viz.

$$T_n^{(ve)}(k, z_1, t) = H(t - t_{1,n}) \int_{-t_{1,n}}^{t-t_{1,n}} T^{(ve)}(k, z_1, t') dt' - H(t - t_{2,n}) \int_{-t_{2,n}}^{t-t_{2,n}} T^{(ve)}(k, z_1, t') dt' \quad (17)$$

or, upon substitution for  $T^{(ve)}$  from Eq. (16),

$$T_n^{(ve)}(k, z_1, t) = [H(t - t_{1,n}) - H(t - t_{2,n})] \left[ T^{(e)}(k, z_1) + \sum_{m=1}^M T_m^{(v)}(k, z_1) \right] - \sum_{m=1}^M \{ H(t - t_{1,n}) \exp[s_m(k)t_{1,n}] - H(t - t_{2,n}) \exp[s_m(k)t_{2,n}] \} \times T_m^{(v)}(k, z_1) \exp[-s_m(k)t]. \quad (18)$$

Here, the transfer functions  $T$  are to be interpreted either as those for displacement,  $W$ , or those for potential,  $G$ .

## Appendix B

### Inverse Hankel transformation of wave-number solutions

For the  $n$ -th box-car loading function, the pressure  $q_n$  exerted at the observation point  $(x, y)$  by an axisymmetric load of parabolic cross-section with axial thickness  $h_{0,n}$ , radius  $R_n$ , density  $\rho$  and centered at the source point  $(x_n, y_n)$  is given by

$$q_n(\Delta r_n) = \rho g h_{0,n} \begin{cases} 1 - (\Delta r_n)^2 R_n^2, & 0 \leq \Delta r_n \leq R_n \\ 0, & R_n < \Delta r_n < \infty \end{cases} \quad (19)$$

where  $(\Delta r_n)^2 = (x - x_n)^2 + (y - y_n)^2$ . If the cross-section is elliptic, this becomes

$$q_n(\Delta r_n) = \rho g h_{0,n} \begin{cases} [1 - (\Delta r_n)^2/R_n^2]^{1/2}, & 0 \leq \Delta r_n \leq R_n \\ 0, & R_n < \Delta r_n < \infty \end{cases} \quad (20)$$

Alternatively,  $q_n$  may be expressed as the zeroth-order Hankel transform, viz.

$$q_n(\Delta r_n) = \int_0^\infty \hat{q}_n(k) k J_0(k \Delta r_n) dk, \quad (21)$$

where

$$\hat{q}_n(k) = \frac{2\rho g h_{0,n}}{k^2} \left[ \frac{2}{k R_n} J_1(k R_n) - J_0(k R_n) \right] \quad (22)$$

for the parabolic cross-section (e.g. Sneddon, 1951, p. 528) and

$$\hat{q}_n(k) = \rho g h_{0,n} R_n^2 \frac{j_1(k R_n)}{k R_n} \quad (23)$$

for the elliptic cross-section (e.g. Terazawa, 1916; Farrell, 1972). The symbols  $J_0$  and  $J_1$  denote the zeroth- and first-order Bessel functions of the first kind. The first-order spherical Bessel function of the first kind,  $j_1$ , can be represented by (e.g. Abramowitz and Stegun, 1965, pp. 437–438)

$$j_1(x) = \left( \frac{\pi}{2x} \right)^{1/2} J_{3/2} = \frac{\sin x}{x^2} - \frac{\cos x}{x}, \quad (24)$$

where  $x$  is an arbitrary argument. With  $W_n^{(ve)}$  or  $G_n^{(ve)}$  given by Eq. (18) and  $\hat{q}_n$  by Eq. (22) or (23), the inverse Hankel transforms

$$w(\Delta r_n, z_1, t) = \int_0^\infty W_n^{(ve)}(k, z_1, t) \hat{q}_n(k) k J_0(k \Delta r_n) dk \quad (25)$$

and

$$\varepsilon(\Delta r_n, z_1, t) = \frac{1}{g} \int_0^\infty G_n^{(ve)}(k, z_1, t) \hat{q}_n(k) k J_0(k \Delta r_n) dk \quad (26)$$

can be evaluated. If there are  $N$  box-car loading functions, superposition gives the total displacement  $w(x, y, z_1, t)$  and the total geoid perturbation  $\varepsilon(x, y, z_1, t)$ .

*Acknowledgements.* The improvements to the manuscript suggested by A.K. Goodacre, A. Lambert and M. Paul are gratefully acknowledged. The reported research was carried out during the tenure of a Canadian Government Laboratory Visiting Fellowship.

## References

- Abramowitz, M., Stegun, I.A., eds.: Handbook of mathematical functions. New York: Dover 1965
- Andersen, B.G.: Late Weichselian ice sheets in Eurasia and Greenland. In: The last great ice sheets, G.H. Denton, T.J. Hughes, eds.: pp. 1–65. New York: John Wiley 1981
- Andrews, J.T.: A geomorphological study of post-glacial uplift with particular reference to Arctic Canada. London: Institute of British Geographers 1970
- Balling, N.: The land uplift in Fennoscandia, gravity field anomalies and isostasy. In: Earth rheology, isostasy, and eustasy, N.-A. Mörner, ed.: pp. 297–321. Chichester: John Wiley 1980
- Bemmelen, R.W. van, Berlage, H.P., jr.: Versuch einer mathematischen Behandlung geotektonischer Bewegungen unter besonderer Berücksichtigung der Undationstheorie. Gerlands Beitr. Geophys. 43, 19–55, 1935
- Bullen, K.E.: An introduction to the theory of seismology, 3rd edn. Cambridge: Cambridge University Press 1963
- Cathles, L.M.: The viscosity of the earth's mantle. Princeton: Princeton University Press 1975
- Daly, R.A.: The changing world of the ice age. New Haven: Yale University Press 1934
- Donner, J.: The determination and dating of synchronous Late Quaternary shorelines in Fennoscandia. In: Earth rheology, isostasy, and eustasy, N.-A. Mörner, ed.: pp. 285–293. Chichester: John Wiley 1980
- Eronen, M.: Late Weichselian and Holocene shore displacement in Finland. In: Shorelines and isostasy, D.E. Smith, A.G. Dawson, eds.: pp. 183–207. London: Academic Press 1983
- Farrell, W.E.: Deformation of the earth by surface loads. Rev. Geophys. Space Phys. 10, 761–797, 1972
- Farrell, W.E., Clark, J.A.: On postglacial sea level. Geophys. J. R. Astron. Soc. 46, 647–667, 1976
- Geer, E.H. de: Skandnaviens geokronologi. Geol. Fören. Stockholm Förh. 76, 299–329, 1954
- Haskell, N.A.: The motion of a viscous fluid under a surface load. Physics 6, 265–269, 1935
- Hyvärinen, H., Eronen, M.: The Quaternary history of the Baltic, the northern part. Acta Univ. Upsala Symp. Upsala Ann. Quing. Cel. 1, 7–27, 1979
- Kääriäinen, E.: The second levelling of Finland in 1935–1955. Publ. Finn. Geod. Inst. 61, 1–313, 1966
- Lidén, R.: Den senkvartära strandförskjutningens förlopp och kronologi i Ångermanland. Geol. Fören. Stockholm Förh. 60, 397–404, 1938
- McConnell, R.K., jr.: Viscosity of the mantle from relaxation time



- spectra of isostatic adjustment. *J. Geophys. Res.* **73**, 7089–7105, 1968
- Nadai, A.: *Theory of flow and fracture of solids*, Vol. 2. New York: McGraw-Hill 1963
- Nansen, F.: The strandflat and isostasy. *Avh. Norske Vid.-Akad. Math.-Naturvid. Kl.* **11**, 1–313, 1921
- Niskanen, E.: On the upheaval of land in Fennoscandia. *Ann. Acad. Sci. Fenn. Ser. A* **53**, 1–30, 1939
- Niskanen, E.: On the deformation of the earth's crust under the weight of a glacial ice-load and related phenomena. *Ann. Acad. Sci. Fenn. Ser. A3* **7**, 1–59, 1943
- Niskanen, E.: On the elastic resistance of the earth's crust. *Ann. Acad. Sci. Fenn. Ser. A3* **21**, 1–23, 1949
- Nye, J.F.: A method of calculating the thickness of the ice-sheets. *Nature* **169**, 529–530, 1952
- Orowan, E.: Contribution to discussion at joint meeting of the British Glaciological Society, the Rheologists' Club and the Institute of Metals. *J. Glaciol.* **1**, 231–236, 1949
- Parsons, B.E.: *Changes in the earth's shape*. Ph. D. thesis. Cambridge: Department of Geodesy and Geophysics, Cambridge University 1972
- Paterson, W.S.B.: *The physics of glaciers*, 2nd edn. Oxford: Pergamon Press 1981
- Peltier, W.R.: The thickness of the continental lithosphere. *J. Geophys. Res.* **89**, 11303–11316, 1984
- Peltier, W.R., Andrews, J.T.: Glacial-isostatic adjustment – 1. The forward problem. *Geophys. J. R. Astron. Soc.* **46**, 605–646, 1976
- Quinlan, G., Beaumont, C.: The deglaciation of Atlantic Canada as reconstructed from the postglacial relative sea-level record. *Can. J. Earth Sci.* **19**, 2232–2246, 1982
- Sabadini, R., Yuen, D.A., Portney, M.: The effects of upper-mantle lateral heterogeneities on postglacial rebound. *Geophys. Res. Lett.* **13**, 337–340, 1986
- Sauramo, M.: Die Geschichte der Ostsee. *Ann. Acad. Sci. Fenn. Ser. A3* **51**, 1–522, 1958
- Sneddon, I.A.: *Fourier transforms*. New York: McGraw-Hill 1951
- Terazawa, K.: On periodic disturbance of level arising from the load of neighbouring oceanic tides. *Phil. Trans. R. Soc. London Ser. A* **217**, 35–50, 1916
- Walcott, R.I.: Isostatic response to loading of the crust in Canada. *Can. J. Earth Sci.* **7**, 716–727, 1970
- Walcott, R.I.: Past sea levels, eustasy and deformation of the earth. *Quat. Res.* **2**, 1–14, 1972
- Walcott, R.I.: Rheological models and observational data of glacio-isostatic rebound. In: *Earth rheology, isostasy, and eustasy*, N.-A. Mörner, ed.: pp. 3–10. Chichester: John Wiley 1980
- Wolf, D.: The relaxation of spherical and flat Maxwell earth models and effects due to the presence of the lithosphere. *J. Geophys.* **56**, 24–33, 1984
- Wolf, D.: The normal modes of a layered, incompressible Maxwell half-space. *J. Geophys.* **57**, 106–117, 1985a
- Wolf, D.: An improved estimate of lithospheric thickness based on a reinterpretation of tilt data from Pleistocene Lake Algonquin. *Can. J. Earth Sci.* **22**, 768–773, 1985b
- Wolf, D.: Glacio-isostatic adjustment in Fennoscandia revisited. *J. Geophys.* **59**, 42–48, 1986a
- Wolf, D.: A method of calculating lithosphere thickness from observations of deglacial land uplift and tilt. *J. Geophys.* **60**, 28–32, 1986b
- Wolf, D.: On deglaciation-induced perturbations of the geoid. *Can. J. Earth Sci.* **23**, 269–272, 1986c
- Wu, P., Peltier, W.R.: Glacial isostatic adjustment and the free air gravity anomaly as a constraint on deep mantle viscosity. *Geophys. J. R. Astron. Soc.* **74**, 377–449, 1983

Received September 15, 1986; revised version April 6, 1987

Accepted April 7, 1987